Earthquake Engineering, Tenth World Conference © 1992 Balkema, Rotterdam. ISBN 90 5410 060 5

Damping factors and resonant frequencies of a nuclear power plant estimated by observed earthquake motion

Katsuhiko Miyazumi, Kosaku Matsuda & Takashi Hosokawa
The Shikoku Electric Power Co., Inc., Japan

Takashi Nishiyama & Nobuaki Katoh
Taisei Corporation, Japan

Tohru Masao
Tajima Engineering Services, Ltd, Japan

ABSTRACT: In order to confirm conditions of the vibration analysis for the Ikata Nuclear Power Station, forced vibration tests and earthquake observation have been carried out. This study is mainly concerned with evaluation of a critical damping ratio of reinforced concrete (RC) material and resonant frequencies of structures using earthquake motions at the Ikata Nuclear Power Station. Five observed earthquakes were used for the study, and the range of their earthquake magnitude was between 4.9 and 7.1. Spectrum ratios exclusive of radiational damping of sway motion were calculated, and simulation analysis was carried out by thin layer method. These results satisfy suitable critical damping ratios and stiffness of structures. From this study, a critical damping ratio of RC material was about 3% for earthquakes of small amplitude, and that of a steel containment vessel was about 2%.

1 INTRODUCTION

Unit No.2 of the Ikata Nuclear Power Station is a PWR type 2-loops 566 MWe plant. Earthquakes have been observed from March of 1982. A simple resonant curve of a structure is obtained by the forced vibration test, but a critical damping ratio of the structure evaluated from the test contains radiation damping because of the small amplitude of the vibration. On the other hand, the critical damping ratio in the range of larger amplitudes than the forced vibration test can be obtained by the observed earthquake motion. In this study, critical damping ratios and stiffness of structures were evaluated from spectrum ratios obtained from earthquake records and simulation analyses by thin layer method. The spectrum ratios of earthquake record were between the basemat and each observed points of the structure. The spectrum ratios of the simulation analysis were between free field surface of the ground and each observed points of the structure.

2 OUTLINE OF STRUCTURE AND GROUND CONDITION

The section of the reactor building of Unit No.2 is shown in Fig.1. Its height is about 75m, the diameter of an outer shield wall(O/S) is 38m. The diameter of a circular basemat is about 42m and the thickness of the basemat is about 14.3m. The structures are located on hard green schist, shear wave velocity was 2.3km/sec. An inner concrete(I/C), O/S and a steel containment vessel (C/V) stand on the circular basemat without connection of each other. The upper portion of O/S makes a half sphere. At the inside of C/V, a crane is installed at the height of 54.65m. As a assumption for response analysis, the weight of the crane was included in a mass point of C/V. Horizontal response analysis did not take account of bending effect of I/C floors which had very large stiffness.

The site ground is hard rock that shear wave velocity is 2.3km/sec. Its Young's modulus is similar to the basemat of the reactor building. The properties of the ground is considered homogeneous. For the analysis, the ground was half-spaced homogeneous media taking 2.3km/sec as shear wave velocity, 3.0ton/m ^{3} as density.

3 OUTLINE OF EARTHQUAKE OBSERVATION AND ITEMS FOR RECORDS

A transducer of earthquake motion was a servo-type accelerometer, and its natural period was 5Hz. Output signals were recorded in an analog data recorder passing low pass filter whose cutting frequency was more than 32Hz. The location of accelerometers is shown in Fig. 1. The direction of vibrational component of eathquake motion for the analysis was Y-Y' in Fig. 1. Acclerometers were also located on the free field surface apart from the reactor building at the distance of 240m. The directions of components on the free field surface were NS and EW, then these directions did not agree with the component of the reactor building. Relation of these components is shown in Fig. 1. Input motions

for the simulation analysis were transformed by equation (1).

$$X(t) = -NS(t)\cos\theta_1 - EW(t)\cos\theta_2$$
$$Y(t) = -NS(t)\cos\theta_2 + EW(t)\cos\theta_1 \quad (1)$$
$$\theta_1 = 0.82 \ , \theta_2 = 0.75$$

Epicentral distances of recorded earthquakes are shown in Fig. 2. Characteristics of recorded earthquakes are shown in Table 1. The range of earthquake magnitude was from 4.9 to 7.1. The maximum acceleration of 25 Gal was observed at the upper surface of the basemat. Recorded earthquake motions were digitalized as a same sampling rate of 0.005 second.

Table 1. Characteristics of earthquakes

	Name of Earthquake	Year Month	Magni-tude	Depth km	Epicen. Dist.	Max Gal
1	Uwakai	'81.7	5.0	60	15	14.4
2	Iyonada	'83.6	4.9	73	35	5.1
3	Ooitaken	'83.8	6.8	116	66	24.4
4	Hyuganada	'84.8	7.1	33	124	9.1
5	Ehimeken	'85.5	6.0	39	60	24.5

4 ESTIMATION OF DAMPING AND NATURAL FREQUENCY BY SPECTRUM RATIO

Spectrum ratios of the structures to the upper surface of the basemat (Point205 in Fig.1) were calculated. Each Fourier spectrum was smoothed using Parzen window of 0.25 wide band. Critical damping ratios were obtained by the method of curve fitting of SDF. The curve fitting method can be carried out by few data near the peak amplitude. On the other hand, the half power method needs many data and the result by this method will contain error due to fluctuation of a spectrum ratio curve. Fig. 3 to Fig.7 show the spectrum ratios of O/S, I/C and C/V respectively in each earthquake. Peak frequencies were found clearly in these figures. As for a special feature in these figures, the natural frequencies of O/S and C/V were found to be nearly equal. The average natural frequencies of O/S and C/V were 7.26 Hz and 7.18Hz respectively, but the average natural frequency of I/C was 11.36Hz, separated from O/S and C/V. Critical damping ratios by the curve fitting method are shown in Table 2, and the values varied with earthquakes. The averages of critical damping ratios in each structure were

I/C(EL32.2m:208Y) = 2.46 %
O/S(EL77.1m:221Y) = 2.68 %
C/V(EL75.1m:213Y) = 1.53 %

Table 2 Critical damping ratios by curve fitting

Position	Height:m	Component	Uwakai	Iyonada	Ooitaken	Hyuganad	Ehimeken
I/C	26.2	206Y	1.45	3.22	2.80	3.81	1.42
	32.2	207Y	1.52	2.99	2.97	3.51	2.70
		208Y	1.93	2.50	2.18	3.16	2.55
O/S	42.4	214Y	2.14	3.38	-	-	-
		215Y	2.44	3.06	-	-	-
	58.1	217Y	2.00	3.68	2.97	3.12	2.25
		218Y	1.91	3.98	2.88	-	2.63
	71.5	220Y	2.36	4.61	-	3.57	-
	77.1	221Y	2.01	3.75	2.65	2.98	2.03
C/V	42.4	210Y	2.36	0.86	-	1.55	1.00
	75.1	213Y	1.89	2.23	1.42	1.08	1.03

unit : %

5 SIMULATION ANALYSIS BY THIN LAYER METHOD

Homogeneous ground under the basemat was divided into 21 layers with the total depth of 167.5m. Ground properties are shown in Table 3. For internal material damping of ground, 2% was adopted.

Table 3. Caluculation constants of ground

Shear wave velocity(m/sec)	2300
Comp. wave velocity(m/sec)	4566
Density (t/m^3)	3.0
Poisson's ratio	0.33
Internal material damping(%)	2.0

The first natural frequency of this ground was 3.43Hz. The analytical model of the superstructure is shown in Fig. 8. The model of O/S was a bending shear bar with 9 mass points. The model of I/C was a bending shear bar of 5 mass points, and the weight of I/C were concentrated in these points at the floor level. The model of C/V was also a bending shear bar of 10 mass points. The basemat was assumed as a rigid solid body. The total weight of the basemat was concentrated at the mass point 11 and mass points 10,18,29 and 12 had no weight. From the concrete strength test, Young's modulus of concrete was 3.8×10^4 MPa and Poisson's ratio was 0.167. Young's modulus of C/V for response analysis was 2.0×10^5 MPa, Poisson's ratio was 0.3.

The result of eigenvalue analysis is shown in Table 4, here mass point 12 was fixed. From this table, the following characteristic

was found that natural frequencies of O/S and C/V were nearly equal. This results agreed with the result by spectrum ratios of observed earthquake motions. Judging from the condition that O/S and C/V were placed near each other to the basemat and the basemat was made of elastic material, vibrational modes of O/S and C/V were supposed to influence each other.

Table 4. Results of eigenvalue analysis

	Fequency Hz	Period sec.	Damping %	Mode
1	6.329	0.158	2.0	C/V
2	6.640	0.150	3.0	O/S
3	12.960	0.077	3.0	I/C
4	18.340	0.055	3.0	O/S 2nd
5	20.340	0.049	2.0	C/V 2nd

The control point for the analysis was located at free field surface 240m away from the reactor building. Spectrum ratios of the analysis were based on this control point. Spectrum ratios of O/S, I/C, C/V and the basemat are shown in Fig. 9 respectively. Analytical results agreed with observed results. Material damping as a complex damping was 3.0% for O/S and I/C which were of RC material and 2.0% for C/V which was of steel. Acceleration time history by the analysis is shown in Fig.10 as compared with the observation at each point. Maximum values of acceleration and time covariance of both analysis and observation agreed with each other.

6 CONCLUSION

The following results were obtained from the analysis of observed earthquake motions.

1) The average damping ratio of O/S made of reinforced concrete material was 2.68%, which was evaluated by five earthquakes. In case of I/C, its value was 2.46%.

2) The average damping ratio of the steel containment vessel was 1.53% which was smaller than the RC structure.

3) Resonant frequencies of the structure obtained by five earthquakes agreed with each other. It is supposed that strain of the structure was small and remained in elastic region.

4) The simulation analysis using thin layer method was carried out. The spectrum ratios of the structures obtained by the observation and the analysis agreed well with each other in the range of first natural frequencies. The result denoted that the values of 3% for O/S and I/C and 2% for C/V as critical damping ratios were appropriate for this analysis. The spectrum ratios by the observation showed the influence of the second vibration mode of each structure in the range of high frequencies, but the spectrum ratios by the analysis did not agree well with the observation. The reason of this was supposed to be the assumption of a rigid solid basement.

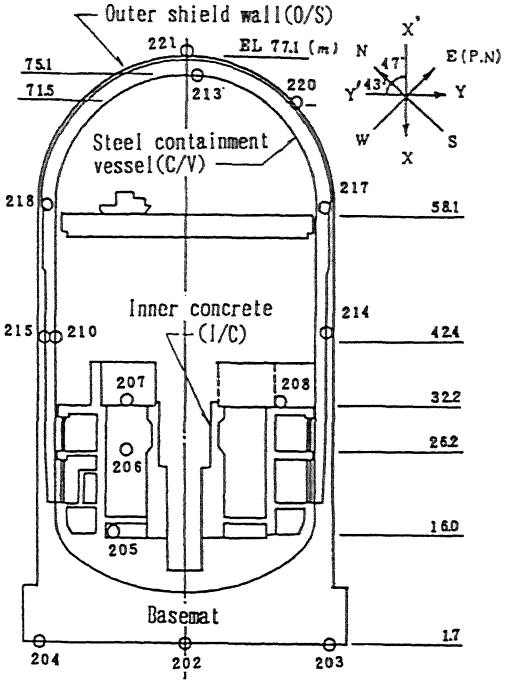

Figure 1 Section of reactor building of Unit No. 2

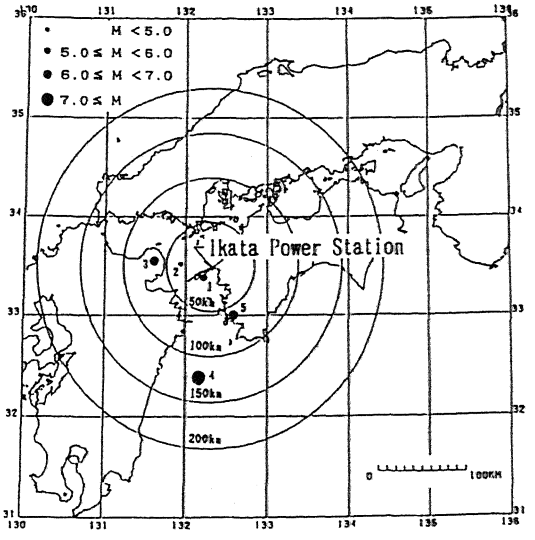

Figure 2 Distribution of epicenter of observed earthquake

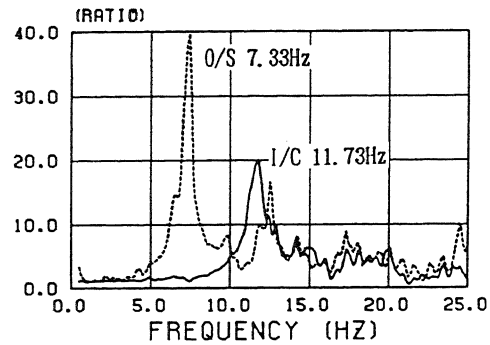

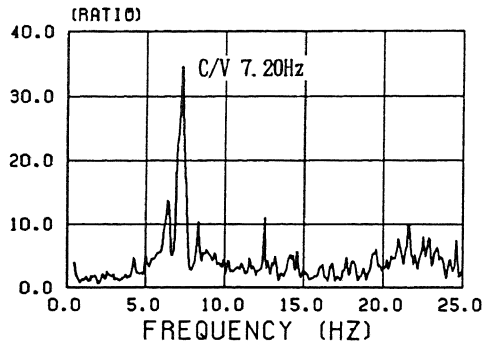

Figure 3 Spectrum ratio of observed earthquake(Uwakai)

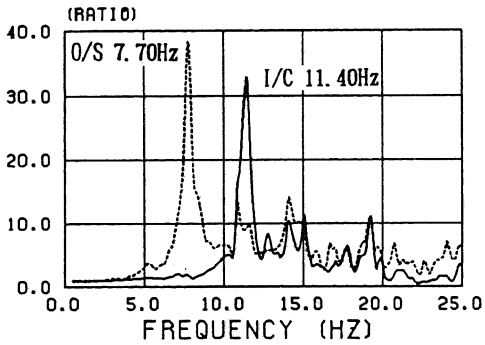

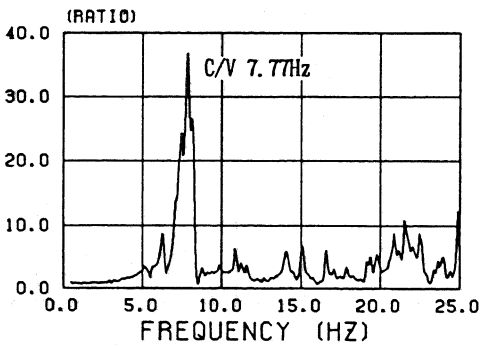

Figure 4 Spectrum ratio of observed earthquake(Iyonada)

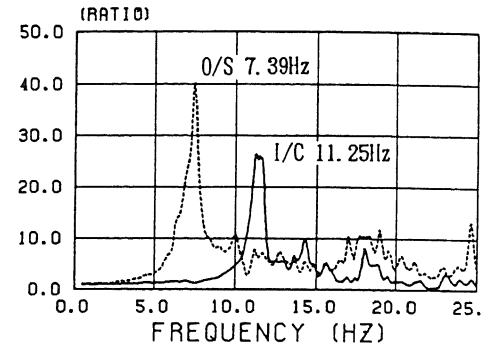

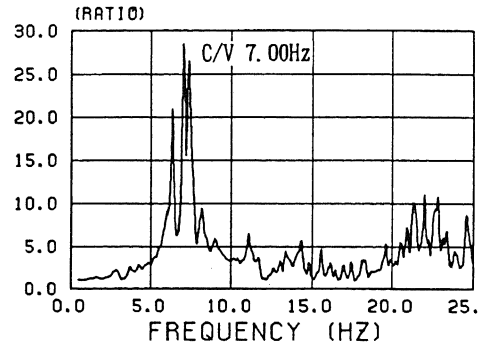

Figure 5 Spectrum ratio of observed earthquake(Ooitaken)

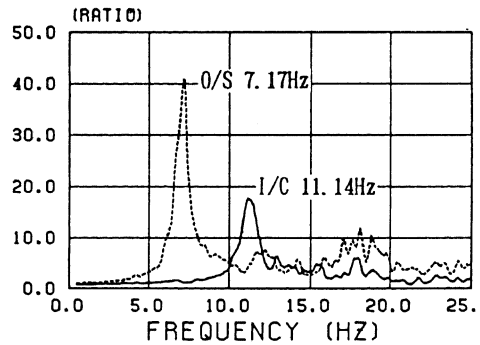

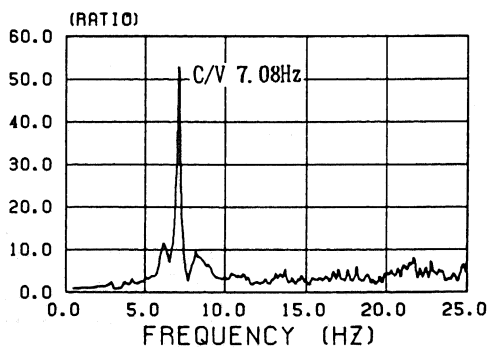

Figure 6 Spectrum ratio of observed earthquake(Hyuganada)

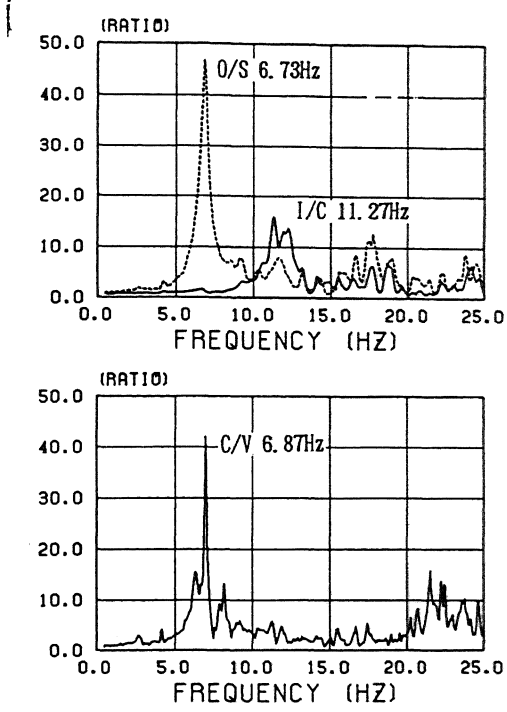

Figure 7 Spectrum ratio of observed earthquake(Ehimeken)

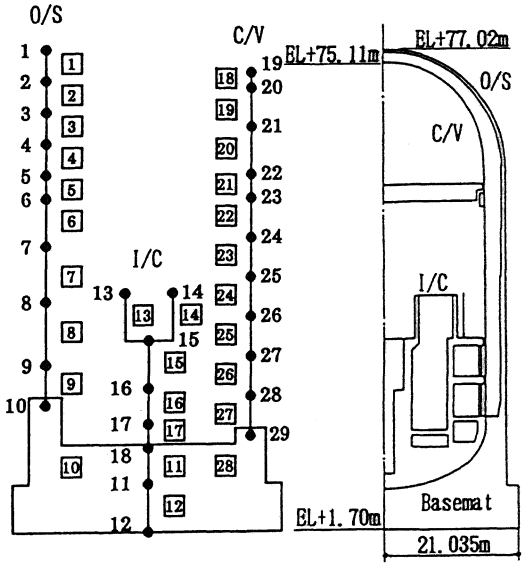

Figure 8 Model for thin layer analysis

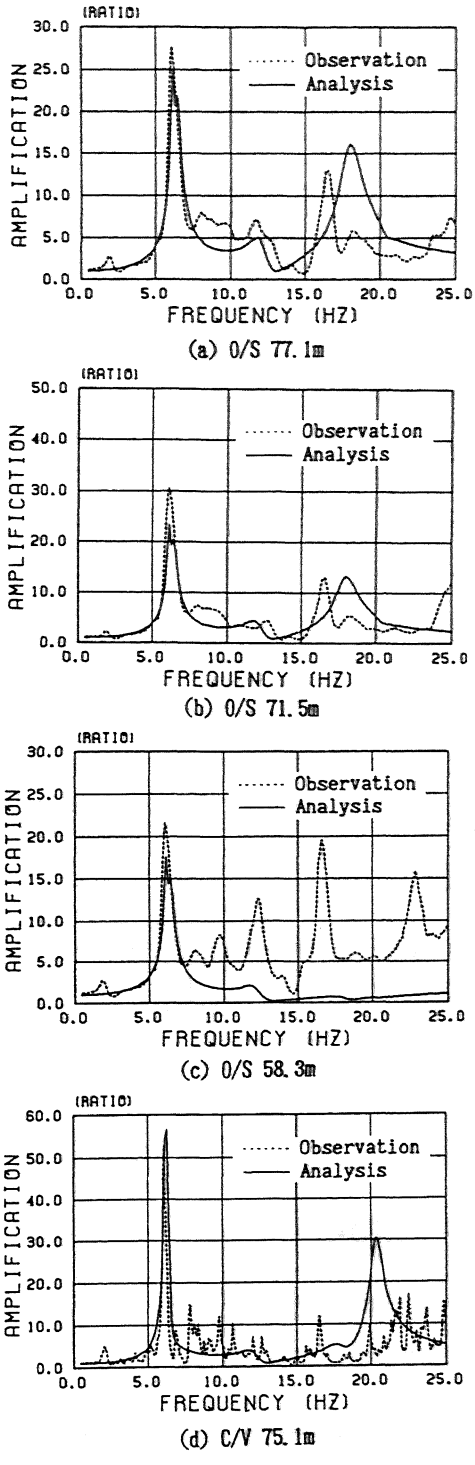

Figure 9 Comparison of spectrum ratio between observation and analysis

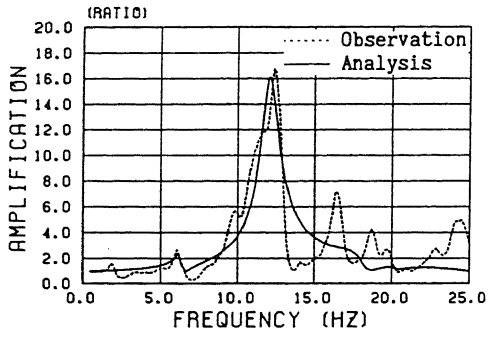

(e) I/C 32.2m

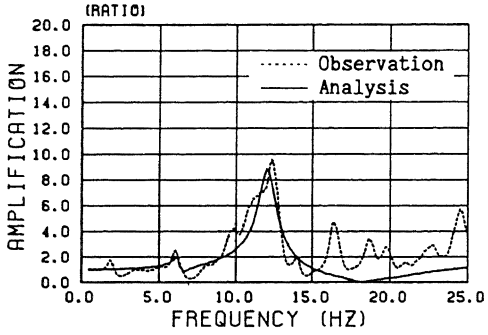

(f) I/C 26.2m

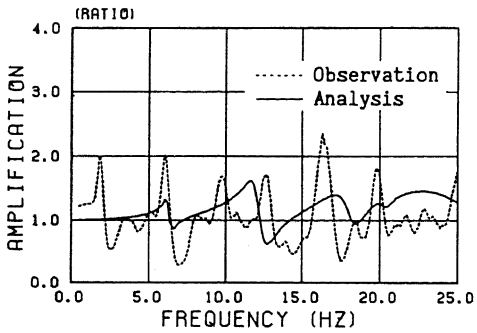

(g) O/S Basemat

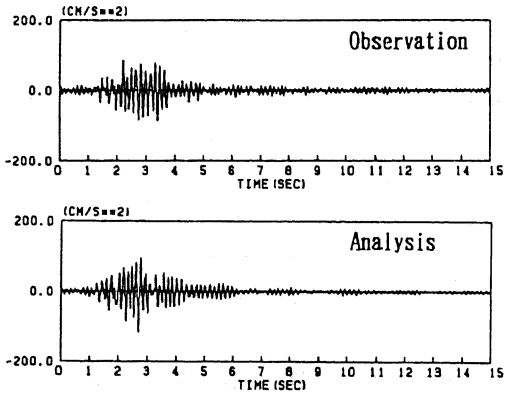

(a) O/S 77.1m

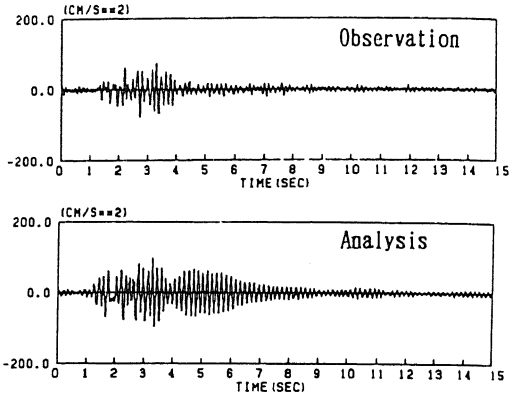

(b) C/V 75.1m

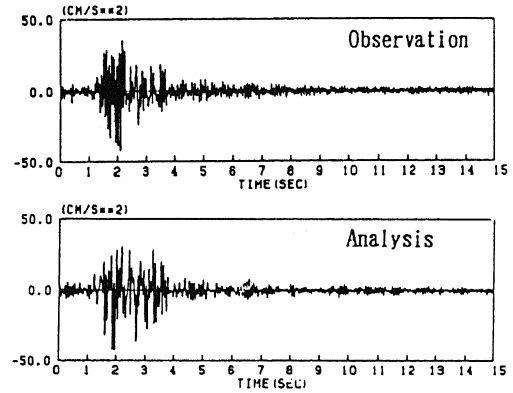

(c) I/C 32.2m

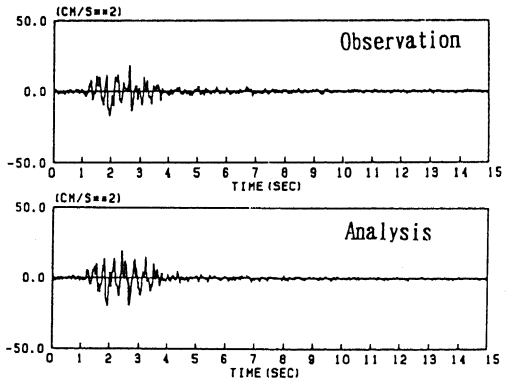

(d) Basemat

Figure 10 Comparison of acceleration time history between observation and analysis